RP Current Trends In Applied Sciences
Vol. 2, No. 4 (October – December 2023) pp. 90–97
e-ISSN: 2583-7486

RESEARCH PLATEAU PUBLISHERS

Cite this article: Ajit Singh, Nonlinear dynamics of acoustic wave propagation in magnetized semiconductor plasmas, *RP Cur. Tr. Appl. Sci.* **2** (2023) 90–97.

Original Research Article

Nonlinear dynamics of acoustic wave propagation in magnetized semiconductor plasmas

Ajit Singh*
Assistant Professor, Department of Physics, Government College, Kalka – 133302 (Panchkula) Haryana, India
*Corresponding author, E-mail: ajitnehra2010@gmail.com

ARTICLE HISTORY
Received: 25 July 2023
Revised: 02 Dec. 2023
Accepted: 05 Dec. 2023
Published online: 08 Dec. 2023

KEYWORDS
Plasma instabilities; Momentum mismatch regime; Piezoelectric semiconductors; Wave propagation behavior; Acoustic gain.

ABSTRACT
The temporal instability of acoustic waves in an unbounded semiconductor plasma is analyzed using a classical hydrodynamic framework. A uniform semiconductor medium subjected to an external magnetic field is considered. The dispersion relations and gain behavior of acoustic waves excited in a piezoelectric semiconductor plasma under conditions of momentum mismatch are investigated. A qualitative numerical study of the four possible propagation modes reveals that a tolerable level of momentum mismatch leads to substantial modification of the acoustic wave spectra. The effects of the applied pump field and the carrier doping concentration on the dispersion and gain characteristics of all supported modes are systematically examined. The findings demonstrate that both the pump field strength and charge carrier density serve as effective control parameters for achieving enhanced propagation and amplification of acoustic waves in the medium. Furthermore, momentum mismatch is shown to increase the phase velocity of strongly unstable modes. These outcomes suggest potential applications in the generation of squeezed states, which are of interest for optical communication systems operating at wavelengths compatible with the spatial scales involved.

1. Introduction

Plasma instabilities arise when key plasma parameters—such as particle density, temperature, electric or magnetic fields, or current—are disturbed from equilibrium. These instabilities strongly affect plasma behavior across different geometrical configurations and operational regimes. Owing to the inherent complexity of the underlying physical mechanisms, effective suppression of plasma instabilities remains a challenging task.

Broadly, the theoretical analysis of plasma instabilities is carried out using two principal approaches. In the first, plasma is modeled as a magnetized hydrodynamic fluid described by a set of fluid equations. In the second, plasma is treated as a statistical ensemble governed by kinetic equations along with suitable distribution functions.

Extensive studies have been reported on the parametric excitation and amplification of acoustic waves in magnetized piezoelectric semiconductor media using the hydrodynamic framework [1,2]. Over the past few decades, considerable attention has been devoted to the investigation of convective amplification and the feasibility of acoustic wave excitation in piezoelectric semiconductor plasmas [3]. Additionally, drift-altered dispersion relations and absorption properties of electro-kinetic waves in non-magnetized extrinsic semiconductors with carrier streaming have been examined [4, 5].

To assess the potential for device realization under varying physical conditions, several studies have explored modifications in the propagation characteristics of longitudinal electro-kinetic waves across different plasma environments [6,7]. Temporal instability of longitudinal electro-kinetic waves has also been analyzed, revealing the emergence of new modes induced by the inclusion of metal nanoparticles within semiconductor plasma media [8].

From an application perspective, the role of density gradients has attracted significant research interest in recent years. Investigations have reported convective amplification or damping, along with propagation characteristics, in both homogeneous and inhomogeneous piezoelectric semiconductor plasma systems [9–11]. Furthermore, second harmonic generation in magnetic media possessing spatially non-uniform magnetization has been examined [12]. A comprehensive theoretical framework for wave propagation in inhomogeneous plasmas was earlier developed by Mikhailovoskii [13]. More recently, Vranjes and Poedts [14] demonstrated that density gradients can lead to noticeable modifications in the ion cyclotron frequency. In addition, the excitation mechanisms and dynamical behavior of nonlinear optical responses in ferroelectric semiconductor crystals have been explored in recent studies [15].

In the studies reported in Refs. [1–12], the propagation of small-amplitude periodic perturbations has been examined using the fundamental equations of the hydrodynamic model. In these analyses, the presence of instability is identified by evaluating the phase relationship of the perturbed quantities. A disturbance is considered to grow in time when the corresponding gain coefficient assumes a positive value. From a practical standpoint, the primary objective is to tailor the field configurations and physical parameters of the system in such a way that the growth rate of the propagating wave is maximized. Consequently, the sign of the gain coefficient serves as the decisive factor in determining the stability or instability of the system.

Plasma instabilities originate from the availability of free energy within the medium, which enables energy exchange between the propagating wave and the plasma. Non-uniform energy distributions and equilibrium currents established by specific geometries or externally applied steady fields can act as natural sources of instability. Alternatively, instabilities may be externally driven by introducing an additional energy source capable of inducing currents in the system. In many cases, a high-intensity beam is employed as a pump field to introduce nonlinearity via nonlinear current densities. This nonlinear interaction leads to coupling among different wave modes through nonlinear polarization, resulting in propagation characteristics that differ markedly from those predicted by linear theory. Energy transfer between coupled waves can occur repeatedly through this mechanism, giving rise to enhanced nonlinear polarization, generation of new frequency components, and significant energy redistribution driven by field-induced distortions of the charge distribution within the medium.

In most previous studies, the pump field has been assumed to be spatially uniform [16,17], and consequently, effects such as local-field corrections and spatial dispersion have received limited attention. For a free-electron system, the second-order susceptibility is zero within the dipole approximation. However, when spatial dispersion is taken into account, a finite, wave-vector-dependent second-order susceptibility emerges due to spatial variations in the electric field and the influence of the Lorentz force [18]. This behavior is well described by the Lorentz–Drude harmonic oscillator model [19,20]. Therefore, instead of assuming a spatially uniform pump field, it is more appropriate to consider a pump field with spatial variation. The inclusion of nonlocal effects necessitates the consideration of spatial dispersion, while the presence of nonlinearity leads to significant modifications in the spectral characteristics of an intense beam propagating through the medium [21].

Although strict momentum conservation is generally desirable for maximizing wave coupling efficiency, the feasibility of achieving exact phase matching through dispersion control in photonic crystals has been theoretically explored [22]. Nevertheless, when analyzing the propagation and evolution of fields in dispersive media, spatial separation effects often give rise to momentum mismatch conditions [23,24]. Under such circumstances, interacting waves periodically drift in and out of phase, resulting in alternating constructive and destructive interference as they propagate through the medium. This highlights the importance of examining the influence of momentum mismatch on plasma wave instabilities. To quantitatively account for this effect, a physical parameter known as the phase mismatch factor, Δk, must be introduced to characterize the extent of phase mismatch between the interacting waves.

Motivated by both earlier and recent developments, the present work focuses on examining the nonlinear nature of temporal instability associated with acoustic wave propagation in a semiconductor plasma medium. The propagation characteristics of acoustic waves are analyzed using a nonlinear dispersion relation that explicitly incorporates momentum mismatch effects. Particular emphasis is placed on understanding how external magnetic fields and momentum mismatch jointly influence and modify the acoustic wave spectrum.

2. Theoretical formulation

This section presents the fundamental equations governing the parametric dispersion relation in a compound semiconductor plasma. To analyze the temporal instability of acoustic waves, we consider the incidence of a longitudinal plane pump mode $E_0 = E_0 \exp[i(k_0 x - \omega_0 t)]$ on a piezoelectric semiconductor plasma subjected to a transverse external magnetic field B_0 directed along the Z-axis. Here, the pump wave is characterized by its wave vector $\vec{k}_0$ and angular frequency ω_0. The interaction of this high-frequency pump wave leads to the parametric generation of a low-frequency acoustic wave (idler mode) along with an electron plasma wave (signal mode). A strong nonlinear coupling between the acoustic wave and the electron plasma wave is anticipated. Under appropriate conditions, these two modes can mutually drive each other unstable by drawing energy from the pump electric field, in accordance with the energy conservation condition
$\omega_1 = \omega_0 - \omega_a$, where ω_1 and ω_a denote the frequencies of the signal (electron plasma) wave and the acoustic wave, respectively.

The propagation characteristics of the acoustic wave are determined through a dispersion relation obtained by solving, in a self-consistent manner, the governing set of equations comprising the momentum transfer equation, Poisson's equation, and the lattice vibration equation.

To investigate the parametric excitation of acoustic waves in the plasma medium, we begin with the following momentum transfer equations:

$$\frac{\partial \vec{v}_0}{\partial t} + \vec{v}_0(\nabla \vec{v}_0) + \nu \vec{v}_0 = \frac{e}{m}[\vec{E}_0 + (\vec{v}_0 \times \vec{B}_0)] \tag{1}$$

$$\frac{\partial \vec{v}_1}{\partial t} + \vec{v}_0(\nabla \vec{v}_0) + \vec{v}_1(\nabla \vec{v}_1) + \nu \vec{v}_1 = \frac{e}{m}[\vec{E}_1 + (\vec{v}_1 \times \vec{B}_0)]. \tag{2}$$

Equations (1) and (2) represent the zeroth-order and first-order momentum balance equations for the oscillating electron fluid. In these equations, m denotes the effective mass of the charge carriers, while ν is the electron collision frequency in the semiconductor plasma, indicating that momentum relaxation is governed by the difference between the mean electron velocities. The quantities E_0 and B_0 correspond to the applied pump electric field and the externally imposed magnetic field, respectively.

$$\frac{\partial n_1}{\partial t} + n_0\left(\frac{\partial v_1}{\partial x}\right) + n_1\left(\frac{\partial v_0}{\partial x}\right) + v_0\left(\frac{\partial n_1}{\partial x}\right) = 0 \tag{3}$$

$$\frac{\partial E_1}{\partial x} + \frac{\beta}{\varepsilon}\left(\frac{\partial^2 u}{\partial x^2}\right) = \frac{n_1 e}{\varepsilon} \tag{4}$$

$$\frac{\partial^2 u}{\partial t^2} + 2\gamma_s\left(\frac{\partial u}{\partial t}\right) + \frac{\beta}{\rho}\left(\frac{\partial E_1}{\partial x}\right) = \frac{C}{\rho}\left(\frac{\partial^2 u}{\partial x^2}\right). \tag{5}$$

Charge conservation in the system is expressed through the continuity equation (3), where n_0 and n_1 denote the equilibrium and perturbed electron number densities. Electrostatic

disturbances arising due to charge separation are governed by Poisson's equation (4), with E_1 representing the space-charge electric field and ε being the dielectric permittivity of the medium. The dynamics of lattice vibrations in the piezoelectric material are described by equation (5), where ρ is the mass density, β is the piezoelectric coupling coefficient, C denotes the elastic constant, and γ_s represents the lattice damping parameter.

From equation (1), the zeroth-order components of the electron fluid velocity along the x and y directions are obtained as follows:

$$v_{0x} = \frac{\bar{E}}{\nu - i\omega_0},\ v_{0y} = \frac{-e\omega_c E_0}{m[(\nu - i\omega_0)^2 + \omega_c^2]},$$

where $\bar{E} = \frac{e}{m}E_0 + \omega_v v_{0y}$ and $\omega_c = \frac{eB_0}{m}$.

The propagation behavior of the acoustic wave under conditions of imperfect momentum matching is analyzed through the introduction of a momentum mismatch parameter, defined as $\Delta k = k_0 - k_1 - k_a$, where k_0, k_1, and k_a represent the wave vectors of the pump, signal, and acoustic waves, respectively. The presence of momentum mismatch introduces additional effects on the propagation and temporal evolution of the interacting fields, which are explicitly incorporated into the present analysis. By differentiating the continuity equation (Eq. (3)) with respect to time and making use of Eqs. (1) – (5), a governing wave equation for the perturbed electron density is obtained as follows:

$$\frac{\partial^2 n_1}{\partial t^2} + \nu\frac{\partial n_1}{\partial t} + \bar{\omega}_p^2 n_1 + \frac{n_0 e\beta R}{m\varepsilon}\frac{\partial^2 u}{\partial x^2} = -i(k_0 + k_1)\left(1 + \frac{\omega_1}{\omega_0}\right)n_1\bar{E} \quad (6)$$

where $\bar{\omega}_p^2 = \omega_p^2 R$, $\omega_p = \left(\frac{n_0 e^2}{m\varepsilon}\right)^{1/2}$, $R = \left(\frac{\omega_1^2}{\omega_c^2 - \omega_1^2}\right)$.

Applying the rotating wave approximation and substituting $n_1 = n_{1f} + n_{1s}$, Eq. (6) can be separated into two distinct components corresponding to fast (n_{1f}) and slow (n_{1s}) parts of the electron density perturbations.

$$\frac{\partial^2 n_{1f}}{\partial t^2} + \nu\frac{\partial n_{1f}}{\partial t} + \bar{\omega}_p^2 n_{1f} = -i(k_0 + k_1)\left(1 + \frac{\omega_1}{\omega_0}\right)n_{1s}^*\bar{E} \quad (7a)$$

$$\frac{\partial^2 n_{1s}}{\partial t^2} + \nu\frac{\partial n_{1s}}{\partial t} + \bar{\omega}_p^2 n_{1s} + \frac{n_0 e\beta R}{m\varepsilon}\frac{\partial^2 u}{\partial x^2} = -i(k_0 + k_1)\left(1 + \frac{\omega_1}{\omega_0}\right)n_{1f}^*\bar{E} \quad (7b)$$

Here, the superscript asterisk (*) denotes the complex conjugate. The fast component corresponds to oscillations at frequencies ($\omega_0 \pm \omega_a$), whereas the slow component oscillates at the acoustic wave frequency ω_a. Assuming a sufficiently long interaction length, only the resonant term ($\omega_0 \pm \omega_a$) is retained, while higher-order harmonics are neglected. Using Eq. (7a) and assuming $\omega_0 >> \omega_a$, the effective fast component of the electron density perturbation can be expressed as:

$$n_f = \frac{-2in_{1s}^*\bar{E}(k_0 + k_1)}{[\bar{\omega}_p^2 - i\nu\omega_0 - \omega_0^2]}\left(1 + \frac{\omega_1}{\omega_0}\right). \quad (8)$$

At this stage, it becomes necessary to formulate the dispersion relation for the acoustic mode by combining Eqs. (5) and (6), which leads to the following acoustic wave dispersion equation:

$$\left(\omega_a^2 + 2i\gamma_s\omega_a - \frac{C}{\rho}k_a^2 - A\right) = \frac{\beta e}{\rho\varepsilon}n_f, \quad (9)$$

where $A = \frac{\beta^2 k_a^2}{\rho\varepsilon}$ is the piezoelectric coupling parameter.

By eliminating n_f and u from Eq. (7b), the generalized modified dispersion relation for the parametric excitation of acoustic waves is obtained:

$$\left(\omega_a^2 - \frac{C}{\rho}k_a^2 - A + 2i\gamma_s\omega_a\right)\left((\bar{\omega}_p^2 - i\nu\omega_a - \omega_a^2) - \frac{2(k_0 + k_1)^2|\bar{E}|^2}{(\bar{\omega}_p^2 - i\nu\omega_0 - \omega_0^2)}\right) = -A\omega_p^2 R \quad (10)$$

The right-hand side of Eq. (10) represents the contribution from the piezoelectric lattice, which serves as a coupling parameter in the system. On the left-hand side, the first term corresponds to the propagation of the acoustic wave in the piezoelectric semiconductor plasma, while the second term accounts for the modified electron plasma wave under the influence of a transverse magnetic field and the momentum mismatch factor Δk, with $k_1 = k_0 - k_a - \Delta k$.

The main objective of this study is to investigate the temporal instability of acoustic waves in a piezoelectric semiconductor plasma medium. Expressing the above relation as a polynomial in terms of the acoustic wave frequency ω_a, we obtain:

$$D_4\omega_a^4 + D_3\omega_a^3 + D_2\omega_a^2 + D_1\omega_a + D_0 = 0 \quad (11)$$

where

$$D_1 = -\left[\frac{C}{\rho}k_a^2\bar{\omega}_p^2 - \frac{C}{\rho}k_a^2\frac{2(k_0 + k_1)^2|\bar{E}|^2}{(\bar{\omega}_p^2 - i\nu\omega_0 - \omega_0^2)}\left(1 + \frac{\omega_1}{\omega_0}\right)^2 + A\bar{\omega}_p^2 - \frac{2A(k_0 + k_1)^2|\bar{E}|^2}{(\bar{\omega}_p^2 - i\nu\omega_0 - \omega_0^2)}\left(1 + \frac{\omega_1}{\omega_0}\right)^2 - \omega_p^2 AR\right],$$

$$D_2 = \left[\frac{C}{\rho}k_a^2 i\nu + Ai\nu + 2i\gamma_s\bar{\omega}_p^2 - \frac{4i\gamma_s(k_0 + k_1)^2|\bar{E}|^2}{(\bar{\omega}_p^2 - i\nu\omega_0 - \omega_0^2)}\left(1 + \frac{\omega_1}{\omega_0}\right)^2\right],$$

$$D_3 = \left[\bar{\omega}_p^2 - \frac{2(k_0 + k_1)^2|\bar{E}|^2}{(\bar{\omega}_p^2 - i\nu\omega_0 - \omega_0^2)}\left(1 + \frac{\omega_1}{\omega_0}\right)^2 + \frac{C}{\rho}k_a^2 + A + 2\gamma_s\nu\right],$$

$D_4 = -[i\nu + 2i\gamma_s]$.

Equation (11) is a fourth-order polynomial, and its roots have been determined using the La Guerre method. Analysis

reveals that the medium, exhibiting second-order nonlinearity, supports four distinct propagation modes. It is evident from Eq. (11) that both the external magnetic field and the momentum mismatch significantly influence the propagation characteristics of all four modes.

3. Results and discussion

Finally, we perform detailed numerical calculations for an n-type CdS piezoelectric semiconductor at 77 K, subjected to a longitudinal plasma mode. The resulting dispersion relation can be used to analyze the acoustic wave spectrum in the semiconductor plasma under conditions of momentum mismatch. Being a fourth-order polynomial, the dispersion relation confirms the existence of four possible acoustic wave propagation channels.

In our analysis, all perturbations are assumed to vary as $\exp[i(kx - \omega t)]$. By separating ω into its real and imaginary parts, $\omega = \omega_{re} + \omega_{im}$, one can identify the nature of wave evolution. If $\omega_{im} > 0$, the wave grows over time, indicating temporal instability by drawing energy from the medium, whereas $\omega_{im} < 0$ corresponds to a decaying wave.

It is important to note that in examining the temporal instability of the acoustic wave with frequency ω_a, the gain characteristics are determined from the imaginary part of ω_a, while the propagation characteristics are associated with the real part.

For the numerical evaluation of our theoretical model, the following parameters are adopted for the n-type CdS piezoelectric semiconductor plasma at 77 K: $m = 0.107m_0$, $\varepsilon_1 = 9.35$, $v_a = 1.8\times10^3$ ms^{-1}, $\beta = 0.21$ Cm^{-2}, $\rho = 4.8\times10^3$ kg m^{-3}, $\omega_0 = 1.78\times10^{14}$ s^{-1}, $\nu = 5\times10^{13}$ s^{-1}, and $\omega_c = 8.21\times10^{11}$ s^{-1}.

It is observed from the solution of polynomial of Eq. (11) that in the absence of momentum matching condition, the semiconductor plasma medium supports four possible modes of propagation. We have investigated the propagation characteristics (in terms of phase velocity V_φ) and gain coefficient of acoustic wave by varying pump electric field E_0 and carrier concentration n_0.

3.1 Effect of spatially dispersive pump field

Considering the experimentally relevant scenario of momentum mismatch, it is important to note that the phase mismatch parameter Δk significantly influences the spatial distribution of the pump field along the sample [25]. Consequently, a spatially dispersive pump field is expected to affect both the gain and propagation characteristics of the acoustic wave. To examine the dependence of the gain and phase profiles on the pump amplitude for all four propagation modes, Figs. 1–4 have been generated.

Figure 1 illustrates the gain behavior of the I and IV Modes as a function of the pump field E_0 for the cases $\Delta k = 0$ and $\Delta k \neq 0$. It is evident from the figure that the I Mode exhibits linear decay, while the IV Mode shows linear growth in both scenarios. Furthermore, the presence of momentum mismatch enhances the attenuation of the I Mode and the amplification of the IV Mode.

Figure 2 shows the variation in the gain profiles of the II and III Modes with changes in E_0 for $\Delta k = 0$ and $\Delta k \neq 0$. These results highlight the role of momentum mismatch in modifying the amplification characteristics of the intermediate modes.

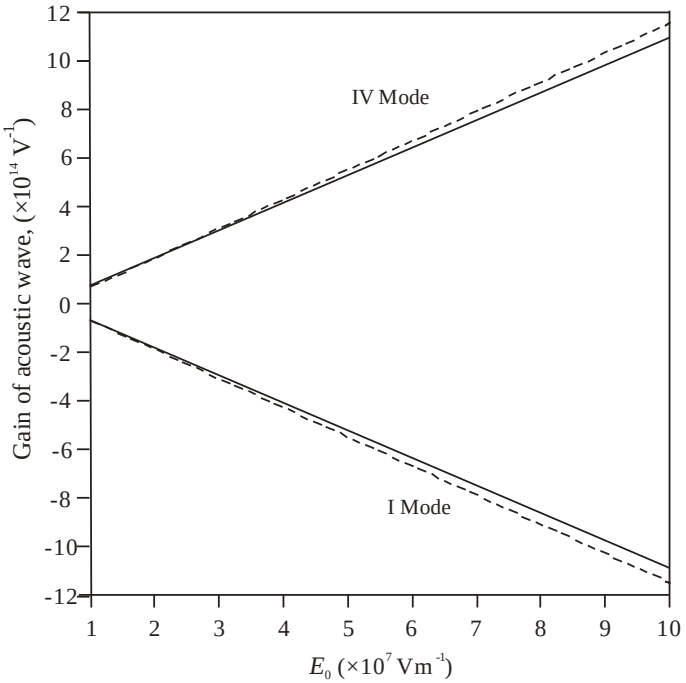

Figure 1: Variation of gain characteristics on pump field for I Mode and IV Mode [$\Delta k = 0$ (solid line), $\Delta k \neq 0$ (dotted line)].

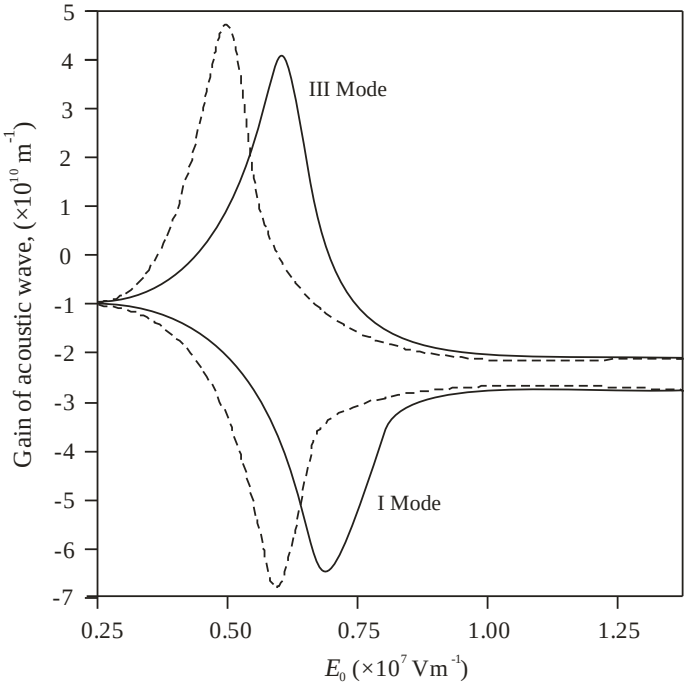

Figure 2: Gain profile of acoustic wave versus pump amplitude for II Mode and III Mode [$\Delta k = 0$ (solid line) and $\Delta k \neq 0$ (dotted line)].

A detailed examination of Fig. 2 indicates that the II Mode exhibits a decaying behavior, while the III Mode generally shows amplification, except within the pump field ranges 0.37×10^7 Vm$^{-1} \leq E_0 \leq 0.65\times10^7$ Vm^{-1} for the phase-mismatched case and 0.42×10^7 Vm$^{-1} \leq E_0 \leq 0.72\times10^7$ Vm^{-1} for the phase-matched scenario. Initially, the attenuation of the II Mode and the amplification of the III Mode increase with the pump amplitude, reaching a maximum at intermediate values. The presence of momentum mismatch enhances this effect, leading to greater attenuation for the II Mode and higher gain for the III Mode compared to the phase-matched case. Beyond $E_0 = 10^7$ Vm^{-1}, the growth rates for all modes become nearly independent of the pump field. Additionally, phase mismatch

causes the locations of the maxima for both modes to shift toward lower values of the pump field.

Figure 3 illustrates the dependence of the phase velocity V_φ on the pump field E_0 for the I and IV Modes. From the figure, it is observed that the I Mode propagates in the opposite direction (contra-propagating), while the IV Mode moves along the same direction as the pump (co-propagating) for both $\Delta k = 0$ and $\Delta k \neq 0$. Initially, the phase velocities of both modes decrease with increasing E_0 up to $E_0 = 10^7$ Vm^{-1}, corresponding to the minimum phase velocity. Beyond this point, further increase in the pump amplitude leads to a linear rise in phase velocity for both modes. Notably, the phase velocities under the momentum mismatch condition ($\Delta k \neq 0$) are slightly higher than those under the phase-matched scenario ($\Delta k = 0$).

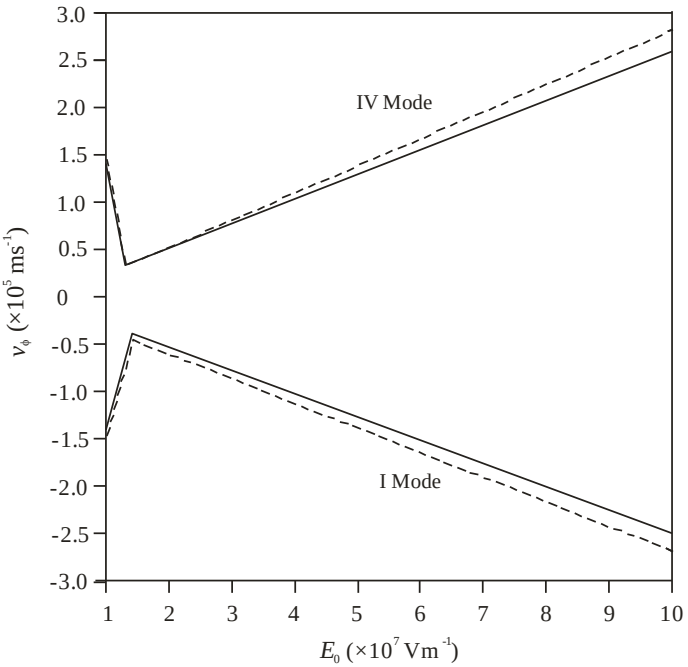

Figure 3: Nature of dependence of phase velocity on pump field for I Mode and IV Mode [$\Delta k = 0$ (solid line) and $\Delta k \neq 0$ (dotted line)].

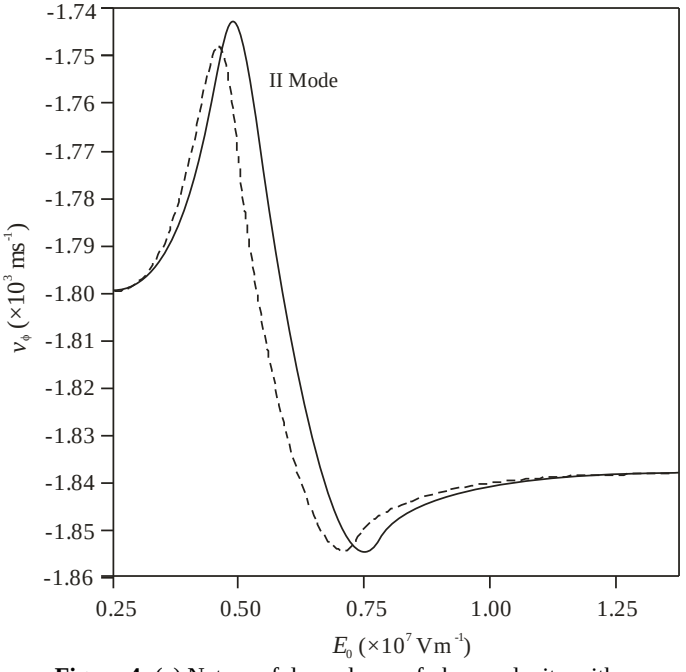

Figure 4: (a) Nature of dependence of phase velocity with pump for II Mode [$\Delta k = 0$ (solid line) and $\Delta k \neq 0$ (dotted line)].

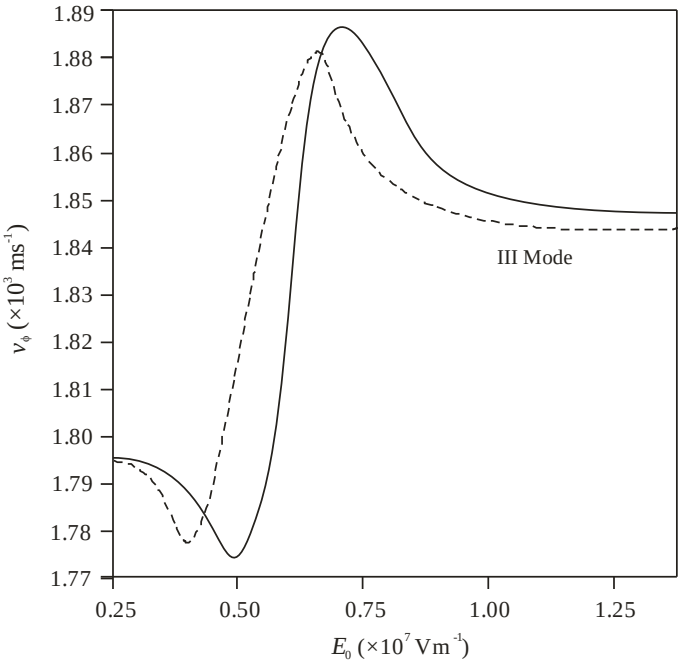

Figure 4: (b) variation of the phase velocity on pump for III Mode [$\Delta k = 0$ (solid line) and $\Delta k \neq 0$ (dotted line)].

The propagation behavior of the II Mode (contra-propagating) and III Mode (co-propagating) is presented in Figs. 4a and 4b as a function of the pump field for both phase-matched and phase-mismatched conditions. Introducing momentum mismatch shifts the locations of the maximum and minimum phase velocities toward lower pump amplitudes. Moreover, the presence of momentum mismatch reduces the phase velocities of both modes compared to the phase-matched case.

3.2 Effect of doping profile of the medium

It is well established that impurities in semiconductors influence both their optical and transport properties [26–28]. Recent studies have shown that, under phase-matching conditions, the intensity of harmonics increases with the carrier density of the medium [29, 30]. Motivated by this, the present work examines the combined effect of phase matching and doping profile on the gain and propagation characteristics of acoustic waves. Figures 5–8 depict these effects for both momentum-matched ($\Delta k = 0$) and momentum-mismatched ($\Delta k \neq 0$) scenarios.

Figure 5 presents the variation of the gain with carrier concentration n_0 for the I and IV Modes under both conditions. It is evident that the I Mode exhibits decay while the IV Mode shows growth for both momentum-matched and mismatched cases. Furthermore, the gain of the IV Mode is higher when momentum mismatch is present, whereas the I Mode experiences greater attenuation under the mismatched condition compared to the matched scenario.

Figure 6 illustrates the gain behavior of the II and III Modes as a function of carrier concentration n_0 for both momentum-matched ($\Delta k = 0$) and momentum-mismatched ($\Delta k \neq 0$) conditions. In both cases, the II Mode remains decaying throughout the considered range, while the III Mode generally decays except within the range 1.4×10^{24} m$^{-3} \leq n_0 \leq 2.7\times10^{24}$ m^{-3}, where it exhibits amplification. This sharp transition in the III Mode highlights a favorable doping range that can serve as an effective control parameter for enhancing amplification. Across

the entire doping range, the presence of momentum mismatch leads to higher values of both attenuation and gain. Specifically, the II Mode shows greater attenuation under momentum mismatch compared to the phase-matched case, whereas the III Mode experiences stronger amplification under mismatched conditions.

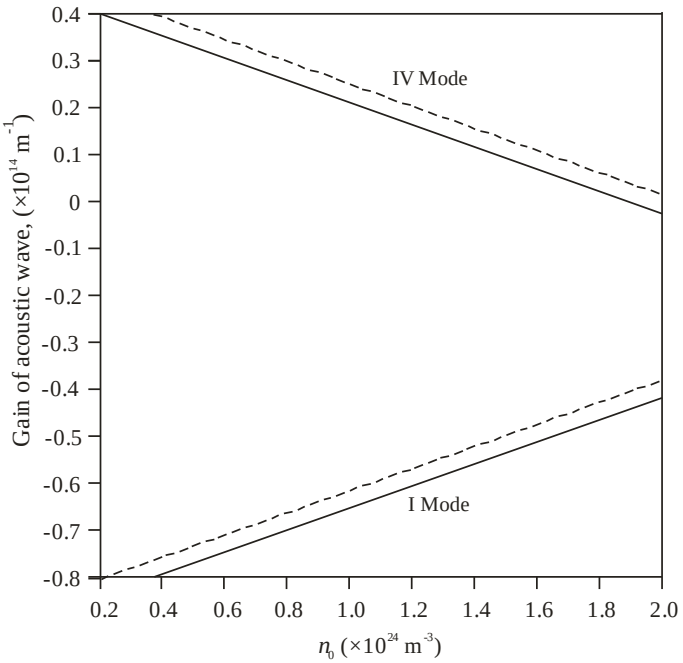

Figure 5: Nature of dependence of gain on carrier density for I Mode and IV Mode [$\Delta k = 0$ (solid line) and $\Delta k \neq 0$ (dotted line)].

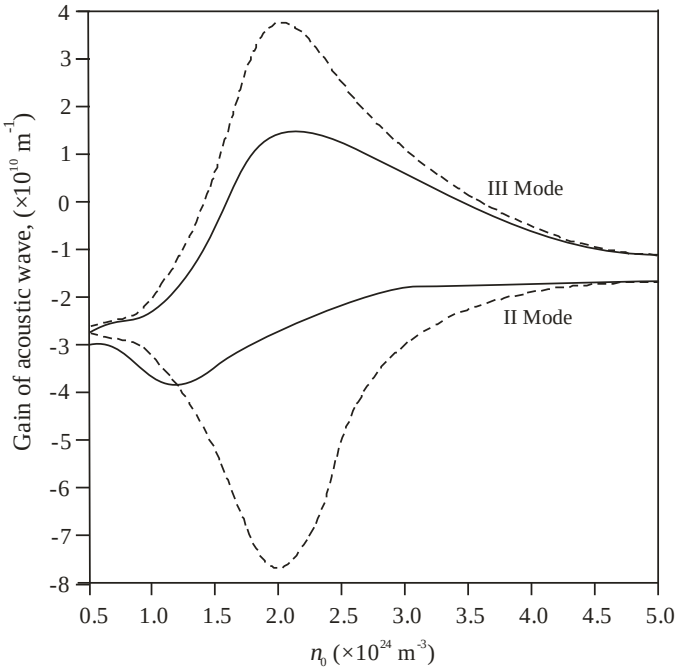

Figure 6: Nature of dependence of gain on carrier density for II Mode and III Mode [$\Delta k = 0$, match (solid line) and $\Delta k \neq 0$, mismatch (dotted line)].

Figure 7 shows the phase velocity behavior of the I and IV Modes as a function of carrier concentration n_0 for both momentum-matched ($\Delta k = 0$) and momentum-mismatched ($\Delta k \neq 0$) conditions. From the figure, it is evident that the I Mode propagates in the opposite direction (contra-propagating), whereas the IV Mode moves along the pump direction (co-propagating) in both scenarios. The phase velocities of both modes decrease with increasing carrier concentration. Additionally, the phase-matched case ($\Delta k = 0$) exhibits slightly higher phase velocities compared to the momentum-mismatched case for both modes.

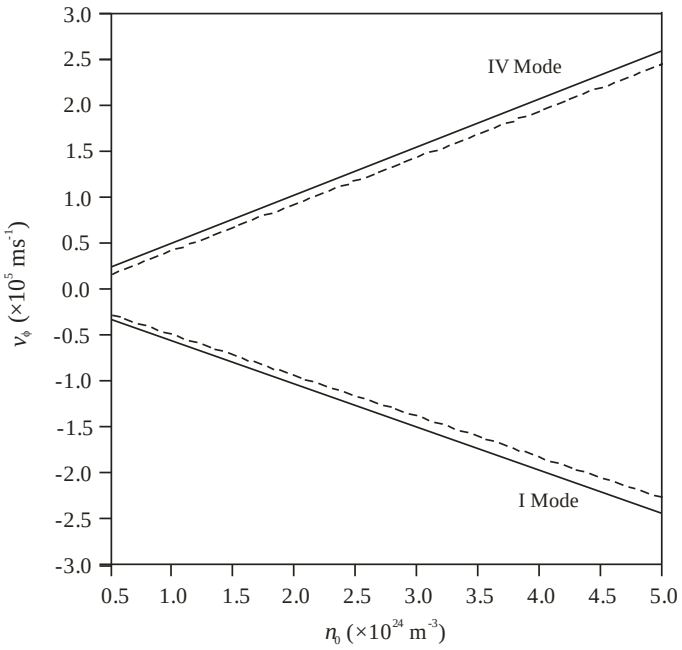

Figure 7: Nature of dependence of phase velocity on carrier concentration for I Mode and IV Mode [$\Delta k = 0$ (solid line) and $\Delta k \neq 0$ (dotted line)].

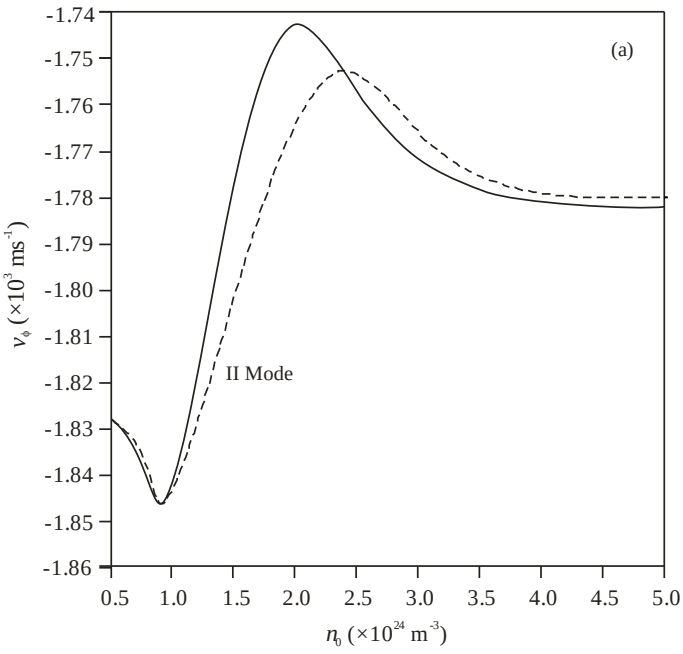

Figure 8: (a) Nature of dependence of phase velocity on carrier concentration for II Mode [$\Delta k = 0$ (solid line) and $\Delta k \neq 0$ (dotted line)]

The phase velocity profiles of the II and III Modes are shown in Figs. 8a and 8b for both momentum-matched ($\Delta k = 0$) and momentum-mismatched ($\Delta k \neq 0$) conditions. It is clear that the II Mode is contra-propagating, while the III Mode is co-propagating in both cases. From Fig. 8a, the phase velocity of the II Mode initially increases similarly for both conditions up to $n_0 = 1\times10^{24}$ m^{-3}, after which it decreases exponentially with

further increases in carrier concentration. The phase velocity under momentum mismatch is observed to be slightly higher than in the phase-matched case. Fig. 8b indicates that the phase velocity of the III Mode rises with increasing carrier concentration, reaching a maximum for both scenarios. Overall, momentum mismatch shifts the positions of maximum and minimum phase velocities toward higher doping concentrations.

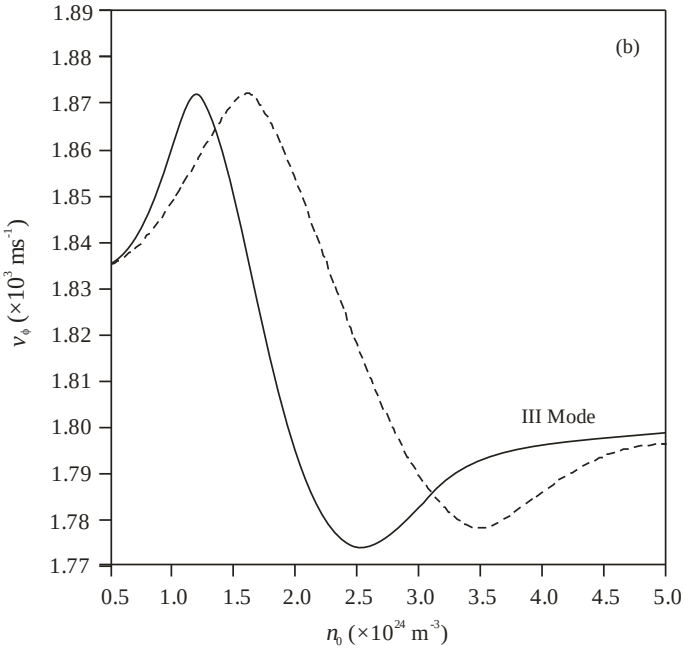

Figure 8: (b) variation of the phase velocity with carrier concentration for III Mode [$\Delta k = 0$ (solid line) and $\Delta k \neq 0$ (dotted line)].

4. Conclusions

We have examined the temporal instability of acoustic waves in a piezoelectric compound semiconductor plasma system. Using a classical hydrodynamic model, the dispersion relation for acoustic waves in a homogeneous semiconductor plasma was derived. The study explores both the propagation and gain characteristics of acoustic waves in a nonlinear optical semiconductor plasma within the classical regime. The analysis confirms that the plasma supports four distinct propagation modes. Numerical calculations for n-type CdS at 77 K indicate that the acoustic gain strongly depends on the pump electric field and the carrier density. The phase velocity profiles show that, under varying spatially dispersive pump field amplitudes, the I and II Modes propagate in the negative X-direction, whereas the III and IV Modes propagate in the positive X-direction, for both momentum-matched and mismatched cases. Furthermore, variations in the pump field reveal that the I and II Modes are decaying, while the III and IV Modes exhibit amplification.

The propagation characteristics of the medium were also analyzed as a function of the doping profile. Among the four modes, the I and II Modes propagate along the negative X-direction, while the III and IV Modes move along the positive X-direction. The gain profile is significantly influenced by variations in the doping concentration, resulting in two decaying modes (I and II) and two amplifying modes (III and IV). Notably, the III Mode exhibits an abrupt transition to amplification within a specific doping range: 1.4×10^{24} – 2.5×10^{24} m^{-3} for the momentum-matched case ($\Delta k = 0$) and 1.7×10^{24} – 2.7×10^{24} m^{-3} for the momentum-mismatched scenario ($\Delta k \neq 0$).

It can be concluded that the momentum mismatch factor (Δk) primarily affects the gain and phase profiles of the acoustic waves in a quantitative manner across all modes, without altering their qualitative behavior. Nevertheless, the combination of varying pump amplitudes and phase mismatch significantly enhances wave–medium interaction, leading to increased growth or attenuation coefficients for all modes. Consequently, the III and IV Modes are found to be highly unstable under tolerable momentum mismatch conditions. Specifically, the presence of Δk increases the phase velocity of the I and IV Modes, while decreasing that of the II and III Modes. In contrast, variations in the doping profile result in higher phase velocities under the momentum-matched condition for the I, III, and IV Modes compared to the mismatched scenario.

Since both the doping profile of the semiconductor plasma and the spatially dispersive pump field act as effective control parameters for the nonlinear temporal instability of acoustic waves under a tolerable phase mismatch, the present results provide valuable insights into the generation and temporal evolution of acoustic waves in direct-bandgap semiconductor plasmas. These findings may also be applied to pump-field squeezing and could offer opportunities to reduce optical signal noise below the vacuum limit in practical photonic or optoelectronic systems.

References

[1] M. Singh, P. Aghamkar, S.K. Bhakar, Parametric dispersion and amplification in semiconductor-plasmas, *Opt. Laser Technol*. **41** (2009) 64–69.

[2] J. Gahlawat, S. Dahiya, M. Singh, High gain coefficient parametric amplification of optical phonon mode in magnetized $A^{III}B^{V}$ semiconductor plasmas, *Arab. J. Sci. Eng*. **46** (2021) 721–729.

[3] M. Singh, M. Singh, Piezoelectric contributions to parametric amplification of acoustical phonons in magnetized n-InSb crystal, *Jordan J. Phys*. **15** (2022) 225–237.

[4] S. Chaudhary, N. Nimje, N. Yadav, S. Ghosh, Drift-modified Longitudinal electro-kinetic wave in colloid laden semiconductor quantum plasmas, *Phys. Res. Int*. **4** (2014) 51.

[5] A. Sharma, N. Yadav, S. Ghosh, Modified acousto-electric interactions in colloids laden semiconductor quantum plasmas, *Int. J. Sci. Res. Pub*. **3** (2013) 1-7.

[6] A. Muley, S. Ghosh, Effect of quantum parameter H on longitudinal electro-kinetic wave characteristics in magnetized semiconductor plasma, *Int. J. Eng. Sci. Res. Tech*. **4** (2015) 88-95.

[7] S. Choudhary, N. Yadav, S. Ghosh, Longitudinal electro-kinetic wave in ion-implanted quantum semiconductor plasmas inpresence of magnetic field, *Int. J. Eng. Sci. Res. Tech*. **4** (2015) 51-57.

[8] S. Ghosh, P. Dubey, Electron-electron two stream instability in embedded assembly of nanoparticle (NP) cluster in n-GaAs, *Can. J. Phys*. **95** (2016) 95-101.

[9] J. Gahlawat, M. Singh, S. Dahiya, Piezoelectric and electrostrictive contributions to optical parametric amplification of acoustic phonons in magnetized doped III–V semiconductors, *J. Optoelectron. Adv. Mater*. **23** (2021) 183–192.

[10] M. Singh, M. Singh, Piezoelectric contributions to optical parametric amplification of acoustical phonons in magnetized doped III–V semiconductors, *Iran. J. Sci. Technol., Trans A: Sci.* **45** (2021) 373–382.

[11] M. Singh, J. Gahlawat, A. Sangwan, N. Singh, M. Singh, Nonlinear optical susceptibilities of a piezoelectric semiconductor magneto-plasma, *Springer Proc. Phys*. **256** (2020) Ch. 20.
[12] E. A. Karashtin, On second-harmonic generation in nonuniformly magnetized media, *Phys. Solid State* **59** (2017) 2189-2197.
[13] A. B. Mikhailovskii, "Most Dangerous" Instabilities of a collision-dominated plasma in a magnetic field, *Sov. Phys. JETP* **25** (1967) 831-838.
[14] J. Vranjes, S. Poedts, Analysis of low-frequency waves in inhomogeneous and bounded plasmas, *Phys. Plasmas* **11** (2004) 891-897.
[15] K.A. Brekhov, K.A. Grishunin, D.V. Afanas'ev, S.V. Semin, N.E. Sherstyuk, E.D. Mishina, A.V. Kimel, Optical second harmonic generation and its photoinduced dynamics in ferroelectric semiconductor $Sn_2P_2S_6$, *Phys. Solid State* **60** (2018) 31-36.
[16] J. Gahlawat, M. Singh, S. Dahiya, Piezoelectric and electrostrictive contributions to optical parametric amplification of acoustic phonons in magnetized doped III–V semiconductors, *J. Optoelectron. Adv. Mater*. **23** (2021) 183–192.
[17] A. Neogi, S. Ghosh, Parametric dispersion and amplification of acousto-helicon waves in piezoelectric semiconductors, *J. Appl. Phys*. **69** (1991) 61-66.
[18] C.S. Wang, *Quantum Electronics, Part A*, H. Rabin and C. L. Tang (Ed.), Academic, New York (1975).
[19] J.A. Armstrong, N. Bloembergen, J. Ducuing, P.S. Pershan, Interactions between light waves in a nonlinear dielectric, *Phys. Rev. Lett*. **127** (1962) 1918-1939.
[20] M. Singh, P. Aghamkar, P.K. Sen, *Simplified modeling of steady-state and transient Brillouin gain*, *Mod. Phys. Lett. B* **21 (2007) 603–614**.
[21] G.S. He, S.H. Liu, *Physics of Non-Linear Optics*, World Scientific, Singapore (1999).
[22] G.M. Savchenko, V.V. Dudelev, V.V. Lundin, A.V. Sakharov, A.F. Tsatsul'nikov, E.A. Kognovitskaya,
[23] S.N. Losev, A.G. Deryagin, V.I. Kuchinskii, N.S. Averkiev, G.S. Sokolovskii, Photonic-crystal waveguide for the second-harmonic generation, *Phys. Solid State* **59** (2017) 1702-1705.
[24] A. Bahabad, M.M. Murnane, C.H. Kapteyn, Quasi-phase-matching of momentum and energy in nonlinear optical processes, *Nat. Photon*. **4** (2010) 570-575.
[25] M.M. Fejer, G.A. Magel, D.H. Jund, R.L. Byer, Quasi-phase-matched second harmonic generation: tuning and tolerances, *IEEE J. Quantum Electron*. **28** (1991) 2631-2654.
[26] Zh. Kudyshev, I. Gabitov, A. Maimistov, Effect of phase mismatch on second-harmonic generation in negative-index materials, *Phys. Rev. A* **87** (2013) 063840.
[27] I. Karabulut, S. Baskoutas, Linear and nonlinear optical absorption coefficients and refractive index changes in spherical quantum dots: Effects of impurities, electric field, size, and optical intensity, *J. Appl. Phys*. **103** (2008) 073512.
[28] R. Turton, *The Quantum Dot — A Journey into the Future of Microelectronics*, Oxford Univ. Press, New York (1995).
[29] G. Bastard, J. A. Brum, R. Ferreira, Electronic states in semiconductor heterostructures, *Phys. Solid State* **44** (1991) 229-415.
[30] P. Balcou, R. Haroutunian, S. Sebban, G. Grillon, A. Rousse, G. Mullot, P. Chambaret, G. Rey, A. Antonetti, D. Hulin, L. Roos, D. Descamps, M.B. Gaarde, A. L'Huillier, E. Constant, et al., High-order-harmonic generation: towards laser-induced phase-matching control and relativistic effects, *Appl. Phys. B* **74** (2002) 509-515.